Neuroprotective effects of *Tiliacora triandra* (Colebr.) Diels leaf extract against lipopolysaccharide-induced memory impairment via anti-neuroinflammation

NAPATR SRIRAKSA[1], SIWAPORN PRAMAN[2], UTCHARAPORN KAMSRIJAI[3,4], ARUNOTHAI WANTA[3,5], SHISANUPONG ANUKANON[4,6], PRACHAK INKAEW[7,8] and THANEEYA HAWISET[2,4]

[1]Department of Physiology, School of Medical Sciences, University of Phayao, Phayao 56000, Thailand; [2]Department of Physiology, School of Medicine, Mae Fah Luang University, Chiang Rai 57100, Thailand; [3]Department of Anatomy, School of Medicine, Mae Fah Luang University, Chiang Rai 57100, Thailand; [4]Integrative Natural Therapeutics and Health Innovation Research Unit (INTHI), Mae Fah Luang University, Chiang Rai 57100, Thailand; [5]Cancer and Immunology Research Center (CIRC), School of Medicine, Mae Fah Luang University, Chiang Rai 57100, Thailand; [6]Department of Pharmacology, School of Medicine, Mae Fah Luang University, Chiang Rai 57100, Thailand; [7]Department of Chemistry, School of Science, Mae Fah Luang University, Chiang Rai 57100, Thailand; [8]Center of Chemical Innovation for Sustainability (CIS), Mae Fah Luang University, Chiang Rai 57100, Thailand

Received October 23, 2025; Accepted March 16, 2026

DOI: 10.3892/br.2026.2148

Abstract. Neurodegenerative diseases are characterized by progressive neuronal loss associated with neuroinflammation. Lipopolysaccharide (LPS) is used as a proinflammatory stimulus in neurodegenerative models, as it induces neuroinflammatory responses and activates microglia and astrocytes, leading to the release of cytokines [such as tumor necrosis factor-α (TNF-α), interleukin (IL)-1β and IL-6] that exacerbate neuronal damage. *Tiliacora triandra*, a medicinal plant native to Southeast Asia, has antioxidant and anti-inflammatory properties. The present study investigated the neuroprotective effects of *T. triandra* leaf extract (TTE) against LPS-induced memory impairment and neuroinflammation in rats. Animals were randomly divided into five treatment groups, namely a vehicle-control, vehicle plus LPS, ibuprofen plus LPS (positive control) and TTE-treated plus LPS groups receiving 200 or 400 mg/kg body weight (BW) TTE for 14 consecutive days. Starting on day 8, LPS (250 μg/kg BW) was administered intraperitoneally for 7 days to induce neuroinflammation. At the end of the treatment period, animals were sacrificed and hippocampal tissues were collected for histological and biochemical analyses. The results demonstrated that TTE significantly ameliorated LPS-induced memory deficits and sickness-like behavior. TTE treatment reduced neuroinflammatory responses, as evidenced by decreased levels of proinflammatory cytokines, such as TNF-α and IL-1β, compared with the vehicle plus LPS group. Additionally, compared with the vehicle plus LPS group, TTE treatment resulted in a reduced number of activated microglia and astrocytes, as indicated by a reduced number of positive cells of ionized calcium-binding adapter molecule 1 and glial fibrillary acidic protein in the hippocampus, respectively. Furthermore, the results of the present study suggested that TTE treatment promoted neuronal survival in hippocampal regions affected by LPS administration. Overall, these findings suggested that TTE mitigated the LPS-induced neuroinflammation and cognitive impairment, which indicates that it may have potential as a therapeutic agent for neuroinflammatory and memory-related disorders.

Correspondence to: Dr Thaneeya Hawiset, Department of Physiology, School of Medicine, Mae Fah Luang University, 333 Moo 1, 1 Phahonyothin Road, Thasud, Muang Chiang Rai, Chiang Rai 57100, Thailand
E-mail: thaneeya.haw@mfu.ac.th

Abbreviations: TTE, *Tiliacora triandra* leaf extract; LPS, lipopolysaccharide; AD, Alzheimer's disease; BW, body weight; GFAP, glial fibrillary acidic protein; Iba1, ionized calcium-binding adapter molecule 1; CA1, cornu ammonis 1; CA3, cornu ammonis 3; DG, dentate gyrus; NF-κB, nuclear factor κ-light-chain-enhancer of activated B cells; COX-2, cyclooxygenase-2; TNF-α, tumor necrosis factor-α; IL-1β, interleukin-1β; YMT, Y-maze test; NORT, novel object recognition test; OFT, open field test

Key words: *Tiliacora triandra*, lipopolysaccharide, memory impairment, neuroinflammation, neuroprotective effect

Introduction

Neuroinflammation is a pathological response of the central nervous system (CNS), which is characterized by the activation of microglia and astrocytes in response to stimuli such as pathogens, toxins or systemic inflammation (1,2). During this process, the activated glial cells promote the inflammatory cascade, identifiable through specific molecular markers, including proinflammatory cytokines [such as tumor necrosis factor-α (TNF-α), interleukin (IL)-1β and IL-6] and cell surface or intracellular markers of glial activation [such as ionized

calcium-binding adapter molecule 1 (Iba1) for microglia and glial fibrillary acidic protein (GFAP) for astrocytes] (3,4).

GFAP is a well-established marker of astrocyte activation and is markedly upregulated during reactive astrogliosis, which involves morphological changes and an increased secretion of inflammatory mediators, such as proinflammatory cytokines, chemokines and reactive molecules (4-6). Astrocyte proliferation is further associated with glial scar formation and the release of proinflammatory factors, such as TNF-α, IL-1β, nitric oxide (NO) and prostaglandin E2, that exacerbate inflammation and disrupt neuronal signaling and synaptic plasticity (3,4,7).

Similarly, Iba1 is a key marker of microglial activation, with increased expression levels as microglia transition from a resting, ramified morphology to an activated, amoeboid form (8,9). Activated microglia secrete proinflammatory cytokines (such as TNF-α, IL-1β and IL-6) and reactive oxygen and nitrogen species, while reactive astrocytes amplify inflammatory signaling and diminish neurotrophic support (9-11). Therefore, elevated GFAP- and Iba1-positive cell populations reflect an increased glial activation, which contributes to neuronal damage and cognitive decline, particularly in hippocampal regions that are important for learning and memory (5,6). Sustained glial activation is associated with the progression of neurodegenerative disorders, such as Alzheimer's disease (AD) and Parkinson's disease (PD) (12,13).

Lipopolysaccharide (LPS), a component of the cell walls of Gram-negative bacteria, triggers a systemic inflammatory response when introduced into the body. LPS binds to Toll-like receptor 4 on immune cells in the periphery. This leads to the release of proinflammatory cytokines, such as TNF-α, IL-1β and IL-6 into the bloodstream (14). These circulating cytokines can then affect the brain through several mechanisms: i) By crossing the blood-brain barrier at regions with higher permeability; ii) by activating endothelial cells to produce secondary inflammatory signals; and iii) by stimulating peripheral nerves. All of these mechanisms result in the activation of microglia and astrocytes within the CNS (14,15). Once activated, these glial cells amplify the inflammatory response by producing additional cytokines and reactive oxygen species (ROS), disrupting synaptic functions, and impairing neuronal signaling. As a result, systemic LPS exposure leads to neuroinflammation, neuronal dysfunction and cognitive deficits, which can be observed in experimental models of neurodegeneration (16,17). Therefore, understanding how natural compounds modulate these inflammatory and glial processes may facilitate the identification of potential therapeutic strategies for cognitive impairment and neurodegeneration.

Tiliacora triandra (Menispermaceae) is a Southeast Asian medicinal plant with well-documented antioxidant and anti-inflammatory activities, which is attributed to its high flavonoid and polyphenol content (18). These bioactive compounds mitigate oxidative stress and suppress key inflammatory mediators, including TNF-α, IL-1β and IL-6 (19). Previous *in vitro* studies demonstrate that *T. triandra* leaf extract (TTE) downregulates inducible NO synthase (iNOS) and cyclooxygenase-2 (COX-2) in LPS-stimulated macrophages (20,21), indicating its potential to counteract LPS-promoted inflammatory cascades. Evidence from animal models of AD, PD, cerebral ischemia-reperfusion injury, as well as studies using alcohol-induced neurotoxicity models, suggests that TTE preserves neuronal survival and supports cognitive function (22-25). However, despite these promising findings, mechanistic data for *T. triandra* are limited compared with other plants such as curcumin and resveratrol. As neuroinflammation, characterized by microglial and astrocytic activation as well as elevated cytokine production, contributes to cognitive decline (5,7,8), the LPS model is relevant when assessing anti-inflammatory and neuroprotective effects. Since it is demonstrated that TTE has a capacity to suppress LPS-responsive inflammatory enzymes and cytokines, the LPS-induced neuroinflammatory model was used in the present study to investigate whether these activities translated into protection at the neurobehavioral, biochemical and histopathological levels. Therefore, the aim of the present study was to investigate whether TTE attenuates LPS-induced cognitive impairments and neuroinflammatory markers, including cytokine expression levels and glial activation, *in vivo*.

Materials and methods

Plant material and preparation of TTE. Fresh *T. triandra* leaves collected from Kantharawichai, Mahasarakham, Thailand, were authenticated by Dr. Napatr Sriraksa. The leaves were then washed with distilled water (DW) for 30 min and dried in a hot-air oven at 60˚C for 72 h before being ground into a fine powder. Aqueous extraction was carried out by boiling the powdered leaves in DW at a 1:5 (w/v) ratio for 10 min. The extract was subsequently filtered through Whatman No. 1 filter paper and concentrated using a rotary evaporator at 50˚C for 2 h (IKA-Werke GmbH & Co. KG). The final concentration of the extract was 6.67% (w/v). The concentrated extract was then freeze-dried at -40 to -50˚C for 6 h using a freeze dryer (Beta 2-8 LSCbasic; Martin Christ Gefriertrocknungsanlagen GmbH) to obtain a dry powder. The extraction yield was 16.67%. The dried extract was stored at -20˚C until use.

Chromatograms and qualitative analyses of compounds in TTE, obtained using liquid chromatography-quadrupole time-of-flight-tandem mass spectrometry, revealed the presence of various chemical constituents, including flavonoids such as catechin, gericudranins A, ambelline, kuwanon Q, tephrowatsin C and armillarivin. Phenolic compounds, including piperine, 6-gingerol, caffeic acid, ilicifolinoside A, salidroside, domesticoside, mahuannin D, leonuriside A and verbascoside, were also identified, as demonstrated in our previous study (22).

Determination of total flavonoid content (TFC). TFC of TTE was determined using the aluminum chloride colorimetric method with minor modifications (26). TTE was diluted to a final concentration of 1,000 μg/ml, and 100 μl of TTE was mixed with 15 μl of 15% (w/w) sodium nitrite and incubated for 6 min at room temperature. Subsequently, 15 μl of 15% (w/w) aluminum chloride was added, followed by an additional 6-min incubation at room temperature, before 70 μl of 8% (w/w) sodium hydroxide was added, and the mixture kept in the dark at room temperature for 15 min. Absorbance was measured at 510 nm, and all measurements were carried out in triplicate. Quercetin standards (500, 250, 125, 62.5 and 31.25 μg/ml) were

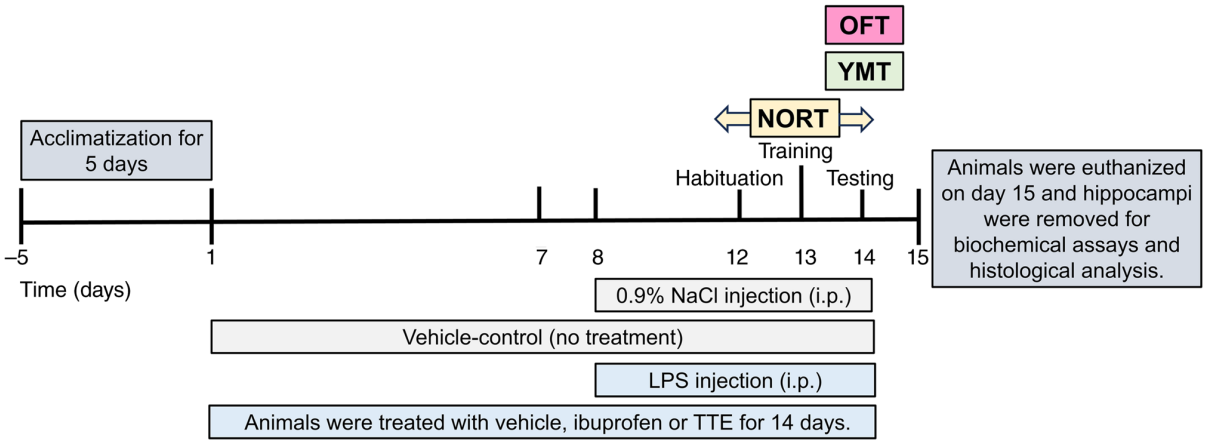

Figure 1. Schematic diagram of the present experimental study. In the present study, animals were orally administered a distilled water vehicle, 50 mg/kg BW ibuprofen or TTE at doses of 200 or 400 mg/kg BW once daily for 14 days. Each group consisted of six animals. From days 8-14, all animals, except for those in the vehicle-control group (which received daily i.p. injections of 0.9% sodium chloride), received daily i.p. injections of 250 μg/kg BW LPS. Behavioral assessments were carried out on day 14 following the final treatment. BW, body weight; TTE, *T. triandra* leaf extract; LPS, lipopolysaccharide; NORT, novel object recognition test; OFT, open field test; YMT, Y-maze test; i.p., intraperitoneal.

used to generate the calibration curve. TFC was calculated from the quercetin acid standard curve and presented as milligrams of quercetin equivalent per gram of TTE (mg QE/g extract).

Determination of total phenolic content (TPC). TPC of TTE was determined using the Folin-Ciocalteu colorimetric assay (26). A 20 μl aliquot of diluted TTE (1,000 μg/ml) was mixed with 100 μl of 0.2 N Folin-Ciocalteu reagent and incubated for 4 min at room temperature. Subsequently, 80 μl of 7.5% (w/v) sodium carbonate was added, and the reaction mixture was incubated in the dark at room temperature for 2 h. Absorbance was measured at 725 nm, and all analyses were carried out in triplicate. Gallic acid standards (500, 250, 125, 62.5 and 31.25 μg/ml) were used to generate the calibration curve. TPC was calculated from the gallic acid standard curve and presented as milligrams of gallic acid equivalent per gram of TTE (mg GAE/g extract).

Animal study. A total of 30 male Wistar rats, aged 8 weeks and weighing between 280-320 g, were sourced from Nomura Siam International Co., Ltd. The sample size for the animal study was determined using G*Power 3.1.9.2 (27,28), based on calculations from a previous study (24). A stratified randomization procedure based on body weight (BW) was used to ensure a balanced allocation of animals across the treatment and control groups. Rats were housed in groups of three per cage under standard laboratory conditions, including a temperature of 22±1˚C, humidity of 35-60% and a 12-h light/dark cycle with free access to food and water throughout the study period. Before behavioral testing, animals were allowed to acclimate to the laboratory environment for 5 days, during which they were also familiarized with the behavioral apparatus. Initial behavioral evaluations were carried out on day 0, with follow-up assessments on day 14. At the start of the experiment, there were no notable differences in locomotor or cognitive performance between the groups, confirming baseline uniformity. Behavioral evaluations included the Y-maze test (YMT), the novel object recognition test (NORT) and the open field test (OFT). Behavioral assessments were conducted by an experimenter who was blinded to the group allocation. Object placement in the NORT and the start arm in the Y-maze were counterbalanced across animals to prevent positional bias.

After completing the final behavioral tests on day 14, the animals were humanely euthanized using an overdose of thiopental sodium on day 15. According to the University of Arizona Guidelines for Anesthetic and Analgesic Use in Laboratory Animals (29), the standard surgical anesthetic dose of thiopental sodium in rats is ~40 mg/kg. The American Veterinary Medical Association guidelines (30) indicate that a euthanasia overdose is typically three times the standard anesthetic dose. Due to variability in individual sensitivity to anesthetic agents, all animals received an initial intraperitoneal injection of thiopental sodium at a dose of 70 mg/kg BW, followed by dose escalation as needed. After administration of the injectable anesthetic, sufficient time was allowed for the animal to lose consciousness. If loss of consciousness was not achieved, additional anesthetic was administered. The absence of the pedal withdrawal reflex was confirmed before sacrifice. The final dose of thiopental sodium used ranged from 70-100 mg/kg BW (31). Cardiac puncture was then used as a secondary method of euthanasia (30). Mortality was confirmed by the absence of a corneal reflex, lack of detectable respiration, absence of a heartbeat and lack of a response to toe pinch. Subsequently, the right hippocampus was dissected for biochemical analysis, while the left hemisphere was collected for histological examination. All experimental procedures were reviewed and approved by the Ethics Committee of the Laboratory Animal Research Center, Mae Fah Luang University (approval no. AR04/67; Chiang Rai, Thailand). An overview of the experimental design is presented in Fig. 1.

Drug administration. Animals were randomly divided into five treatment groups (n=6), namely a vehicle-control, vehicle plus LPS, 50 mg/kg BW ibuprofen (IBU) plus LPS, 200 mg/kg BW TTE plus LPS and a 400 mg/kg BW TTE plus LPS group. Regarding TTE concentrations, the doses were selected based on preliminary neuroprotective and subacute toxicity

studies to identify non-toxic levels and to cover pharmacologically relevant ranges (18,19,22-25). For example, a previous subacute toxicity study reports no abnormalities when treating rats with aqueous extract from *T. triandra* at doses of 300, 600 and 1,200 mg/kg BW for 90 days compared with a control group (32). The concentrations of TTE used in the present study corresponded to levels shown to exert neuroprotective and cognitive-enhancing effects in our previous research (22,23) or were based on effective concentrations reported in the literature (22-24). Since neuroinflammation mimics pathological features of neurodegenerative diseases such as AD, IBU was used as an anti-inflammatory drug to reduce inflammation and protect against the cognitive deficits observed in AD. Therefore, the dosage of IBU was selected based on a previous report indicating its effectiveness for anti-inflammatory, cognitive-enhancing and neuroprotective activities in a rat AD model (33). All treatments were administered orally once daily at 9:00 a.m. for 14 consecutive days. The vehicle-control and vehicle plus LPS group received DW as the vehicle. IBU powder, used as a positive control for its anti-inflammatory and cognitive-enhancing effects, was obtained from Sigma-Aldrich; Merck KGaA. On day 8 of the experiment, the vehicle-control group received an intraperitoneal injection of 0.9% sodium chloride daily for 7 consecutive days, whereas the remaining treatment groups received daily intraperitoneal injections of LPS (Sigma-Aldrich; Merck KGaA) at a dose of 250 μg/kg BW for 7 consecutive days to induce neuroinflammation and cognitive impairment (17,34,35). The animals received either 0.9% sodium chloride or LPS 1 h after oral administration of DW, IBU or TTE. Wistar rats, a widely used outbred albino strain in biomedical research (including infectious disease and toxicology studies) exhibit dose-dependent inflammatory and physiological responses following the intraperitoneal administration of LPS (36-39).

Behavioral tests of the animals

YMT. Spontaneous alternation behavior was assessed using the YMT to evaluate the spatial working memory and exploratory behavior of the animals (40). The Y-maze consisted of three arms, each ~50 cm long and 10 cm wide, with walls 30 cm high. The arms were arranged at 120˚ angles, and the lighting was maintained at ~40 lux. Animals were habituated to the maze for 5 min/day for 5 consecutive days. This test relied on the natural tendency of rodents to investigate unfamiliar arms of the maze, reflecting their cognitive ability to remember previously visited locations. Each animal was placed at the center of the Y-maze and allowed to freely investigate all three arms for 5 min. An arm entry was recorded when all four paws of the animal entered an arm. The sequence of arm entries was used to calculate the percentage of spontaneous alternations, which was defined as successive entries into the three different arms (for example, ABC, BCA and CAB). The percentage of spontaneous alternation behavior was calculated using (40): Spontaneous alternation (%)=[(number of alternations)/(total number of arm entries - 2)] x100. This measure provided an index of short-term spatial memory performance.

NORT. Cognitive performance was assessed using the NORT, which was carried out in a clear Plexiglas box measuring 40x40x40 cm, under constant lighting conditions of ~40 lux. The test consisted of three phases, namely habituation, training and testing (41). During the habituation phase, animals were allowed to freely explore the empty testing arena for 5 min to become accustomed to the environment. Subsequently, 24 h after habituation, during the training phase, two identical objects were placed in the arena, and each animal was permitted to explore for 5 min. During the testing phase, which was carried out 24 h after the training phase, one of the familiar objects was replaced with a novel object, and the animals were again allowed to explore for 5 min. Object exploration was defined as the animal sniffing or directing its nose toward an object within a distance of <2 cm. The time spent exploring each object was recorded, and the discrimination index (DI; a measure of recognition memory) was calculated using: DI (%)=[(T(novel) - T(familiar))/(T(novel) + T(familiar))] x100. T(novel) indicates the time spent exploring the novel object, and T(familiar) indicates the time spent exploring the familiar object.

OFT. An OFT is a behavioral assay used for assessing exploratory activity and general locomotor behavior in rodents (42). The apparatus consisted of a clear Plexiglas box measuring 40x40x40 cm and was maintained under constant lighting conditions of ~40 lux. The box was subdivided into 16 equal squares to facilitate the quantification of movement. Each animal was placed in the center of the arena and allowed to explore freely for 5 min. Locomotor activity was recorded using a video camera, and exploratory behavior was quantified by counting the number of squares crossed, defined as the animal moving into a square with all four paws. The frequency of rearing behavior (when the animal stood upright on its hind legs to explore the box) was also recorded.

Measurement of TNF-α and IL-1β levels. After the animals were euthanized, the right hippocampus was isolated and stored at -80˚C for later biochemical assays. The tissue samples were weighed and homogenized in ice-cold PBS using a glass homogenizer. The resulting homogenates were centrifuged at 10,000 x g for 10 min at 4˚C, and the supernatants were collected and stored at -80˚C until further analysis. To quantify the levels of proinflammatory cytokines, including TNF-α and IL-1β, enzyme-linked immunosorbent assay (ELISA) kits were used, namely rat TNF-α ELISA kit and rat IL-1β ELISA kit (cat. nos. E-EL-R2856 and E-EL-R0012, respectively; Elabscience Bionovation Inc.) were used according to the manufacturer's protocols. The experiment was carried out using six independent biological replicates (n=6/group). To ensure technical reliability, all ELISA assays for each biological sample were carried out in duplicate, and the mean values were used for statistical analysis.

Tissue processing and Nissl staining. After the animals were euthanized, the left cerebral hemispheres were dissected and fixed in 4% paraformaldehyde prepared in 0.1 M PBS (pH 7.4) at 4˚C for 24 h. Following fixation, the tissues were embedded in paraffin and sectioned at a thickness of 5 μm using a Leica RM 2245 rotary microtome (Leica Microsystems GmbH). Paraffin-embedded brain sections were heated at 60˚C and deparaffinized through sequential immersion in xylene, a graded ethanol series and DW for 5-min/step. Nissl staining

was performed using 1% cresyl violet solution (Sigma-Aldrich; Merck KGaA) to highlight neuronal cell bodies, at room temperature for 5 min. After staining, the sections were rinsed twice with DW, dehydrated through a series of ascending ethanol concentrations (70-100%), and cleared in xylene (three changes). Finally, a cover slip was placed over the sections using distyrene, plasticizer and xylene mounting medium (Sigma-Aldrich; Merck KGaA).

Images of the hippocampal subregions [cornu ammonis (CA)1, CA3 and the dentate gyrus (DG)] were obtained at x20 magnification using an Olympus EP50 digital light microscope integrated with EPview imaging software (version 1.4; Olympus Corporation). Neuronal quantification was carried out by an investigator blinded to the treatment groups to reduce potential assessment bias. The number of surviving neurons was measured in each hippocampal area. To ensure consistency in evaluating Nissl-stained sections, three micrographs were analyzed for each hippocampal subregion per animal.

Immunofluorescence staining. Tissue sections were deparaffinized through three successive immersions in xylene, followed by gradual rehydration using a descending ethanol series comprising two changes of 100% ethanol, then 95, 90, 80 and 70% ethanol. Antigen retrieval was conducted by treating the sections with 0.2 M Tris-HCl buffer and autoclaving at 95˚C for 15 min. After cooling to room temperature, the slides were washed twice with PBS. Permeabilization was achieved by incubating the sections in 0.1% Triton X-100 for 15 min, followed by an additional PBS wash. To block non-specific antibody binding, the samples were incubated with 5% BSA (Sigma-Aldrich; Merck KGaA) in PBS at room temperature for 30 min, then rinsed again with PBS.

The sections were then incubated overnight at 4˚C with primary antibodies, namely anti-GFAP monoclonal antibody (1:200; cat. no. MA5-12023; Thermo Fisher Scientific, Inc.) or anti-Iba1 monoclonal antibody (1:200; cat. no. AB178846; Abcam). Subsequently, corresponding secondary antibodies were applied for 1 h at room temperature using goat anti-mouse IgG H&L conjugated to Alexa Fluor® 594 (1:300; cat. no. AB150116; Abcam) and donkey anti-rabbit IgG H&L conjugated to Alexa Fluor® 488 (1:400; cat. no. AB150073; Abcam). After PBS washing, Hoechst 33258 nuclear stain (1:2,000; Abcam, Cambridge, UK) was applied at room temperature for 10 min. Finally, the slides were washed three times with PBS (3 min/wash), mounted using anti-fade fluorescence mounting medium (cat. no. AB104135; Abcam) and sealed with nail polish. Fluorescent images were visualized using a fluorescence Zeiss Axio Scope A1 microscope (Carl Zeiss AG).

To evaluate astrocyte and microglial activation, the number of GFAP- and Iba1-positive cells in the CA1, CA3 and DG regions were quantified. Three brain samples were randomly selected from each experimental group, and 10 sections per sample were analyzed. In total, 30 images per group were captured at x20 magnification using the Zeiss Axio Scope A1 microscope. The number of microglia and astrocytes was assessed by an investigator blinded to the treatment groups to minimize potential assessment bias. Hoechst 33258 (blue) labels the nuclei of all types of cells, including neurons and glial cells. Hippocampal neurons are characterized by larger, diffusely stained nuclei arranged in a dense and organized laminar pattern, whereas glial cells (microglia and astrocytes) exhibit smaller, intensely stained (punctate) nuclei that co-localize with Iba1 or GFAP immunoreactivity (43,44).

Statistical analysis. Statistical analyses were carried out using SPSS Statistics version 25 (IBM Corp.). Data were presented as mean ± standard error of the mean. All data met the assumptions of normality, as assessed using the Shapiro-Wilk test. One-way analysis of variance (ANOVA) was used to assess differences among group means, followed by Tukey's Honestly Significant Difference (HSD) post hoc test for multiple comparisons. Effect sizes (Cohen's d) and 95% confidence intervals were calculated where appropriate, and the distinction between biological and technical replicates was maintained. A two-way mixed ANOVA was used to examine the effects of a between-subjects factor and a within-subjects (repeated-measures) factor on a continuous dependent variable, while also evaluating whether the effect of one factor varied as a function of the other. $P<0.05$ was considered to indicate a statistically significant difference.

Results

TTE contains high levels of flavonoids. Using the aluminum chloride colorimetric method, TTE had a TFC of 30.08 mg QE/g extract. This indicated that flavonoids constitute a major phenolic class within TTE. By contrast, the Folin-Ciocalteu assay showed a TPC of 0.020 mg GAE/g extract. This suggested there was a low concentration of phenolic acids or associated compounds detectable by the Folin reagent.

TTE improves body weight and locomotor activity in LPS-induced sickness-like behavior. LPS is a neurotoxin that induces neuroinflammation and sickness-like behavior, which is characterized by a reduced appetite, decreased locomotion and weight loss (45). In the present study, BW changes following 0.9% sodium chloride (vehicle-control) or LPS injection were analyzed using a two-way mixed ANOVA. There were significant effects for time and the group-by-time interaction (both Wilks' lambda and Greenhouse-Geisser, $P<0.001$). Trend analysis revealed both significant linear ($P<0.001$) and quadratic components ($P<0.01$), confirming that mean BW followed a non-linear, quadratic trajectory over the six measurement points. While the interaction between the linear trend and group was significant ($P<0.001$), the quadratic trend interaction was not ($P=0.413$). Furthermore, the analysis revealed a significant main effect of the experimental group on the measured outcome ($P<0.001$). Post hoc Tukey's HSD comparisons revealed that all LPS-treated animals exhibited a significant reduction in BW compared with the vehicle-control ($P<0.01$); however, no significant differences in weight were observed among the various LPS-treated groups (Fig. 2A). These findings further suggest that LPS administration induces sickness-like behavior, accompanied by reduced BW in the animals.

Additionally, animals treated with vehicle plus LPS had significantly reduced locomotor activity, which was demonstrated by a decrease in the number of times the animals reared ($P<0.01$) and crossed ($P<0.001$) compared

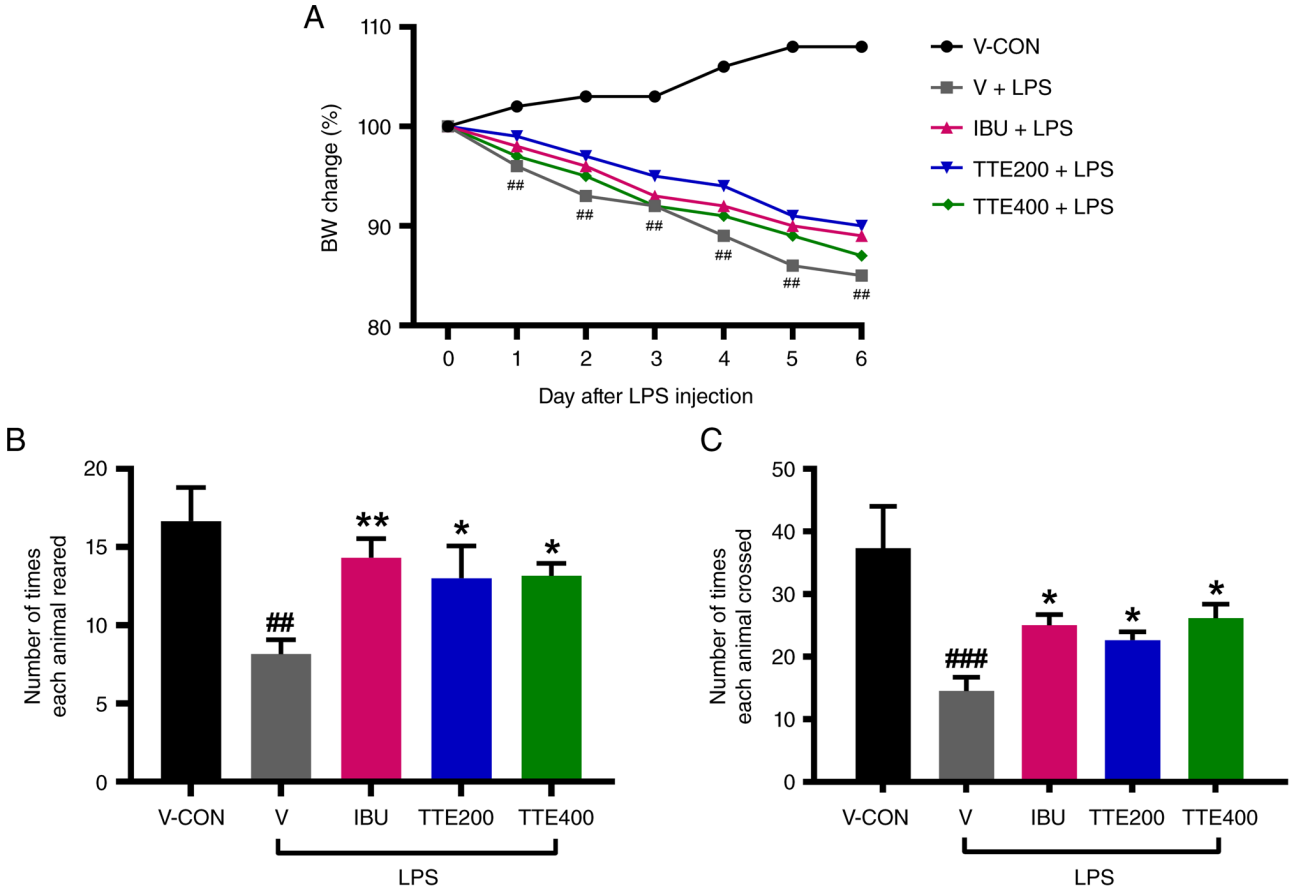

Figure 2. Effect of TTE on BW and locomotive behavior. (A) Percentage of BW change (analyzed using two-way mixed ANOVA). Number of times each animal (B) reared or (C) crossed (analyzed using one-way ANOVA). The data is presented as the mean ± SEM (n=6). $^{\#\#}$P<0.01 and $^{\#\#\#}$P<0.001 vs. the V-CON group. *P<0.05 and **P<0.01 vs. the V plus LPS group. BW, body weight; TTE, *T. triandra* leaf extract; LPS, lipopolysaccharide; V-CON, vehicle-control; V, vehicle; IBU, ibuprofen.

with the vehicle-control group (Fig. 2B and C, respectively). Treatment with IBU or TTE at doses of 200 or 400 mg/kg BW significantly increased the number of times the animals reared (P<0.01, P<0.05 and P<0.05, respectively) and crossed (P<0.05 for all treatment groups) compared with those in the vehicle plus LPS group. Therefore, this indicated that TTE treatment mitigated the sickness-like behavior that was induced by LPS, which may suggest its potential protective or therapeutic effects.

TTE enhances cognitive performance. LPS is widely used in experimental models to induce neuroinflammation and cognitive decline by mimicking features of neurodegenerative diseases (45). Therefore, cognitive function was assessed using cognitive tests, including the YMT and the NORT. In the NORT, vehicle plus LPS-injected animals demonstrated a significant reduction in the discrimination index (P<0.01) compared with the vehicle-control group, as shown in Fig. 3A. However, LPS-injected animals treated with IBU or TTE at doses of 200 or 400 mg/kg BW demonstrated a significant increase in the discrimination index (P<0.01, P<0.05 and P<0.05, respectively) compared with the vehicle plus LPS group.

Additionally, vehicle plus LPS-injected animals had a significant decrease in the percentage of spontaneous alternation behavior (P<0.01) in the YMT, compared with the vehicle-control group (Fig. 3B). However, animals injected with LPS and treated with IBU or TTE at a dose of 400 mg/kg BW showed increased spontaneous alternation behavior (P<0.05 for all treatment groups), compared with the vehicle plus LPS group. These findings suggested that TTE treatment may prevent LPS-induced memory impairment.

TTE reduces proinflammatory cytokine levels. LPS, a component of the outer membrane of Gram-negative bacteria, is a potent inducer of proinflammatory cytokines (such as IL-1β, IL-6 and TNF-α), which induces an acute inflammatory response (19). TNF-α and IL-1β are cytokines produced primarily by activated microglia and astrocytes. Both serve notable roles in the pathophysiology of various neurodegenerative diseases (such as AD and PD) and contribute to the inflammatory responses in the CNS (46). Fig. 4A and B illustrate that animals in the vehicle plus LPS group had significantly higher levels of TNF-α (P<0.001) and IL-1β (P<0.001) compared with the vehicle-control group. By contrast, LPS-injected animals treated with IBU or TTE at doses of 200 or 400 mg/kg BW showed reduced levels of TNF-α (P<0.001 for all treatment groups) and IL-1β (P<0.05 for all treatment groups) compared with the vehicle plus LPS group. These findings suggested that TTE may potentially protect against LPS-induced neuroinflammation by reducing the levels of proinflammatory cytokines.

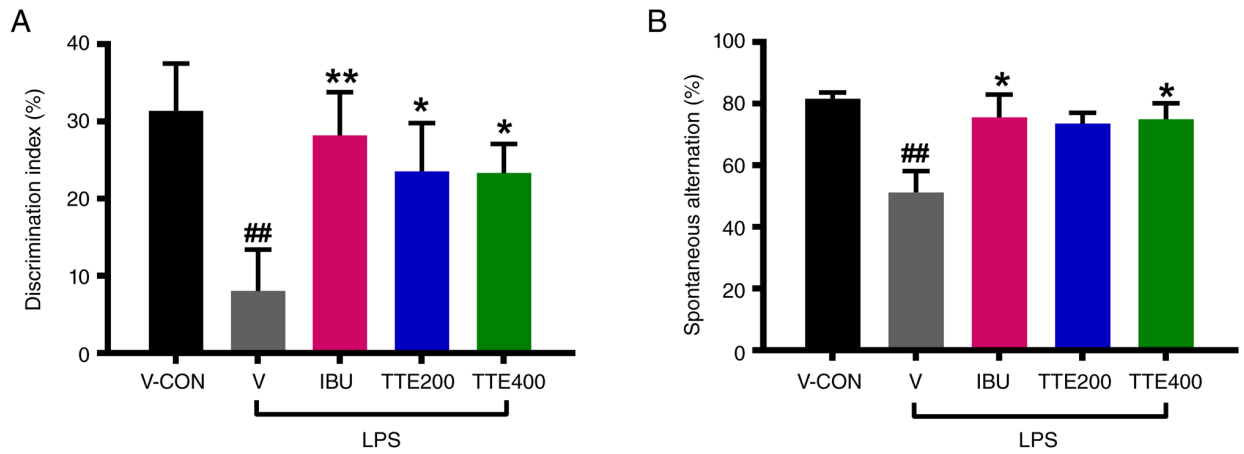

Figure 3. Effect of TTE on cognitive performance. (A) Discrimination index (%). (B) Spontaneous alternation (%). One-way ANOVA was used to analyze the data, and the data is presented as the mean ± SEM (n=6). ##P<0.01 vs. the V-CON group. *P<0.05 and **P<0.01 vs. the V plus LPS group. TTE, *T. triandra* leaf extract; LPS, lipopolysaccharide; V-CON, vehicle-control; V, vehicle; IBU, ibuprofen.

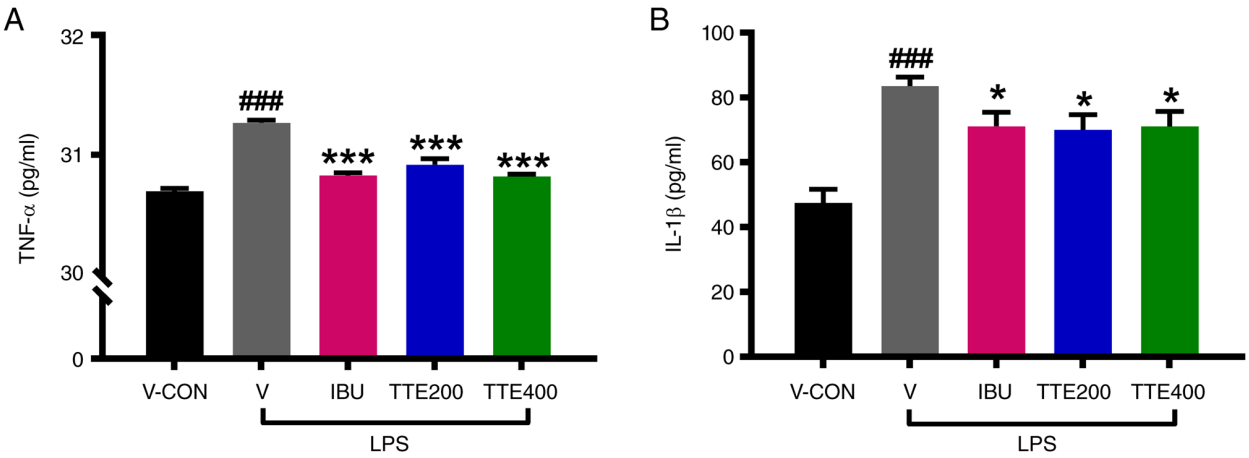

Figure 4. Effect of TTE on proinflammatory cytokines. (A) TNF-α. (B) IL-1β. One-way ANOVA was used to analyze the data, and the data is presented as the mean ± SEM (n=6). ###P<0.001 vs. the V-CON group. *P<0.05 and ***P<0.001 vs. the V plus LPS group. TTE, *T. triandra* leaf extract; LPS, lipopolysaccharide; V-CON, vehicle-control; V, vehicle; IBU, ibuprofen; TNF-α, tumor necrosis factor-α; IL-1β, interleukin-1β.

TTE promotes neuronal survival in the hippocampus. Neuronal survival was evaluated using Nissl staining, which labels Nissl bodies (aggregates of rough endoplasmic reticulum and ribosomal RNA). In healthy neurons, Nissl bodies are abundant and appear as darkly stained granules, reflecting a functional and structurally intact state. By contrast, neuronal injury leads to the dissolution or fragmentation of Nissl bodies, whereas their reappearance indicates recovery or survival. Accordingly, a high density of Nissl-stained neurons is indicative of neuronal preservation, whereas a reduced density or absence of staining reflects neuronal damage or loss (47-49). The Nissl-stained section of the rat hippocampus and the neuronal density in the CA1, CA3 and DG regions is shown in Fig. 5A-D, respectively. Compared with the vehicle-control animals, those in the vehicle plus LPS group had a marked reduction in neuronal survival in the CA1, CA3 and DG regions (P<0.001 for all areas). However, LPS-injected animals that received IBU or TTE (at 200 or 400 mg/kg BW) showed an increased neuronal survival in the CA1 (P<0.01, P<0.01 and P<0.05, respectively), CA3 (P<0.05, P<0.01 and P<0.01, respectively) and DG (P<0.001, P<0.01 and P<0.05, respectively), compared with the corresponding vehicle plus LPS groups. Nissl staining was used to capture micrographs of the CA1, CA3 and DG sections of the hippocampus at a x20 magnification, as shown in Fig. 5E-G, respectively.

TTE reduces the number of Iba1- and GFAP-positive cells in the hippocampus. Iba1 expression levels serves as an indicator of the presence and activation of microglia, the resident immune cells of the CNS. Microglia serve a crucial role in CNS immune defense, responding to injury, infection and neurodegenerative processes (8). In the present study, animals in the vehicle plus LPS group demonstrated a significantly increased number of Iba1-positive cells in the hippocampal CA1, CA3 and DG regions (P<0.001 for all areas) compared with vehicle-control animals, as shown in Figs. 6A, 7A and 8A. By contrast, treatment with IBU or TTE at doses of 200 or 400 mg/kg BW resulted in a significant reduction in number of Iba1-positive cells in the CA1 region (P<0.01, P<0.05 and P<0.01, respectively), CA3 region (P<0.05 for all treatment groups) and DG region (P<0.01, P<0.05 and P<0.05, respectively), compared with the vehicle plus LPS group.

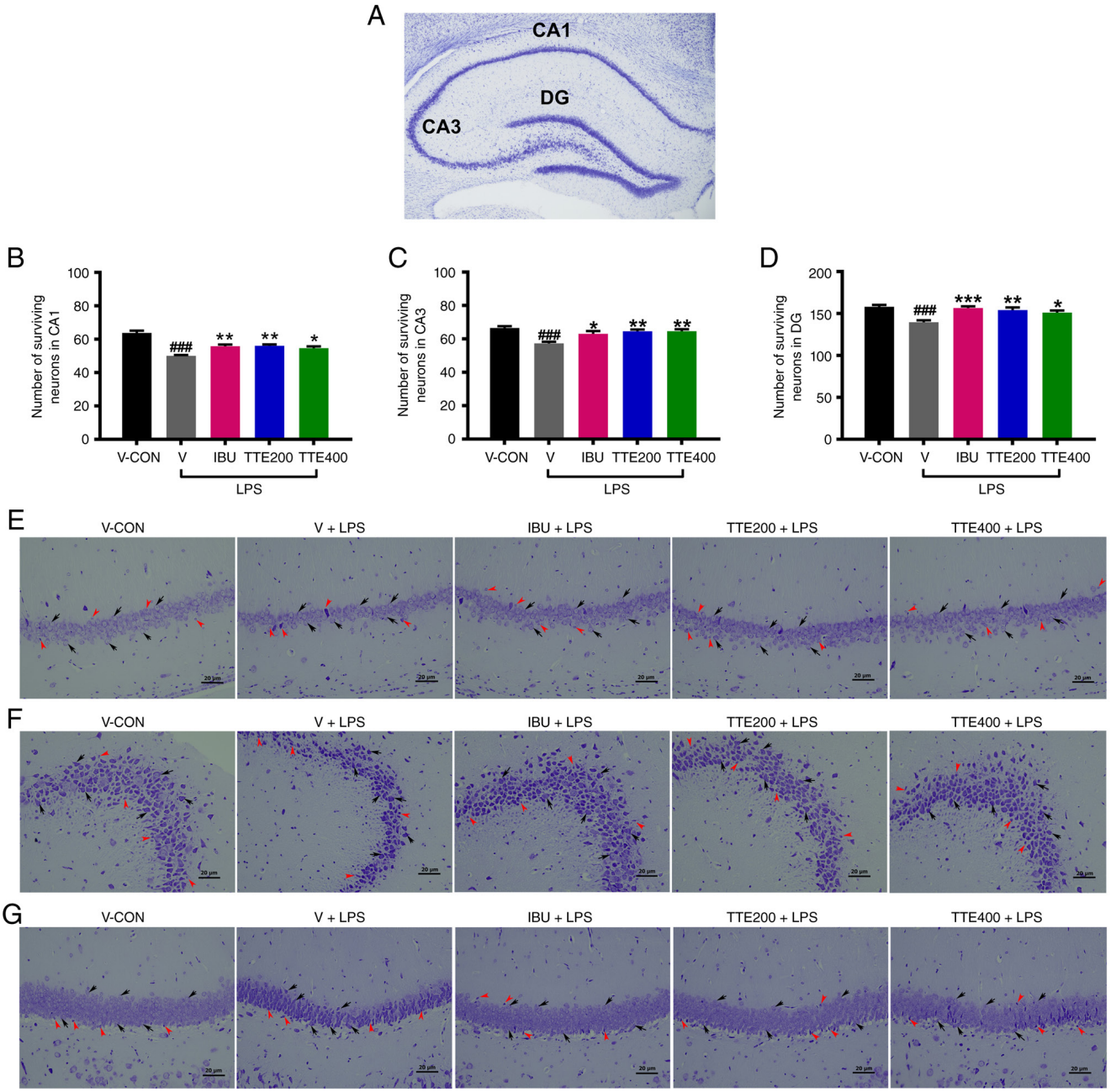

Figure 5. Effect of TTE on the number of surviving neurons in the hippocampus. (A) Nissl-stained section of the rat hippocampus. Number of surviving neurons in the (B) CA1, (C) CA3 and (D) DG. Micrographs of the (E) CA1, (F) CA3 and (G) DG sections of the hippocampus at 20x magnification (scale bar, 20 μm). The red arrowheads indicate the dark, shrunken and damaged neurons. The black arrows indicate the neurons that were still alive. One-way ANOVA was used to analyze the data, and the data is presented as the mean ± SEM (n=6). $^{###}$P<0.001 vs. the V-CON group. *P<0.05, **P<0.01 and ***P<0.001 vs. the V plus LPS group. TTE, *T. triandra* leaf extract; LPS, lipopolysaccharide; V-CON, vehicle-control; V, vehicle; IBU, ibuprofen; CA1/3, cornu ammonis 1/3; DG, dentate gyrus.

GFAP is a well-established marker of astrocyte activation, with its expression levels notably upregulated during reactive astrogliosis (a process characterized by morphological changes in astrocytes and the secretion of inflammatory mediators) (7). In the present study, compared with the vehicle-control group, animals in the vehicle plus LPS group showed a significant increase in the number of GFAP-positive cells in the CA1, CA3 and DG regions of the hippocampus (P<0.001 for all areas), as shown in Figs. 6B, 7B and 8B. However, LPS-injected animals treated with IBU or TTE at doses of 200 or 400 mg/kg BW demonstrated a significant reduction in the number of GFAP-positive cells in the CA1 region (P<0.01, P<0.05 and P<0.05, respectively), CA3 region (P<0.01, P<0.01 and P<0.05, respectively) and DG region (P<0.001, P<0.05 and P<0.05, respectively), compared with the vehicle plus LPS group.

Figs. 6C, 7C and 8C show the immunofluorescence staining of Iba1, while Figs. 6D, 7D and 8D present the immunofluorescence staining of GFAP in the hippocampus at a x20 magnification. Iba1 serves as a specific marker for identifying microglia, whereas GFAP is a specific marker for astrocytes (4-6,8,9).

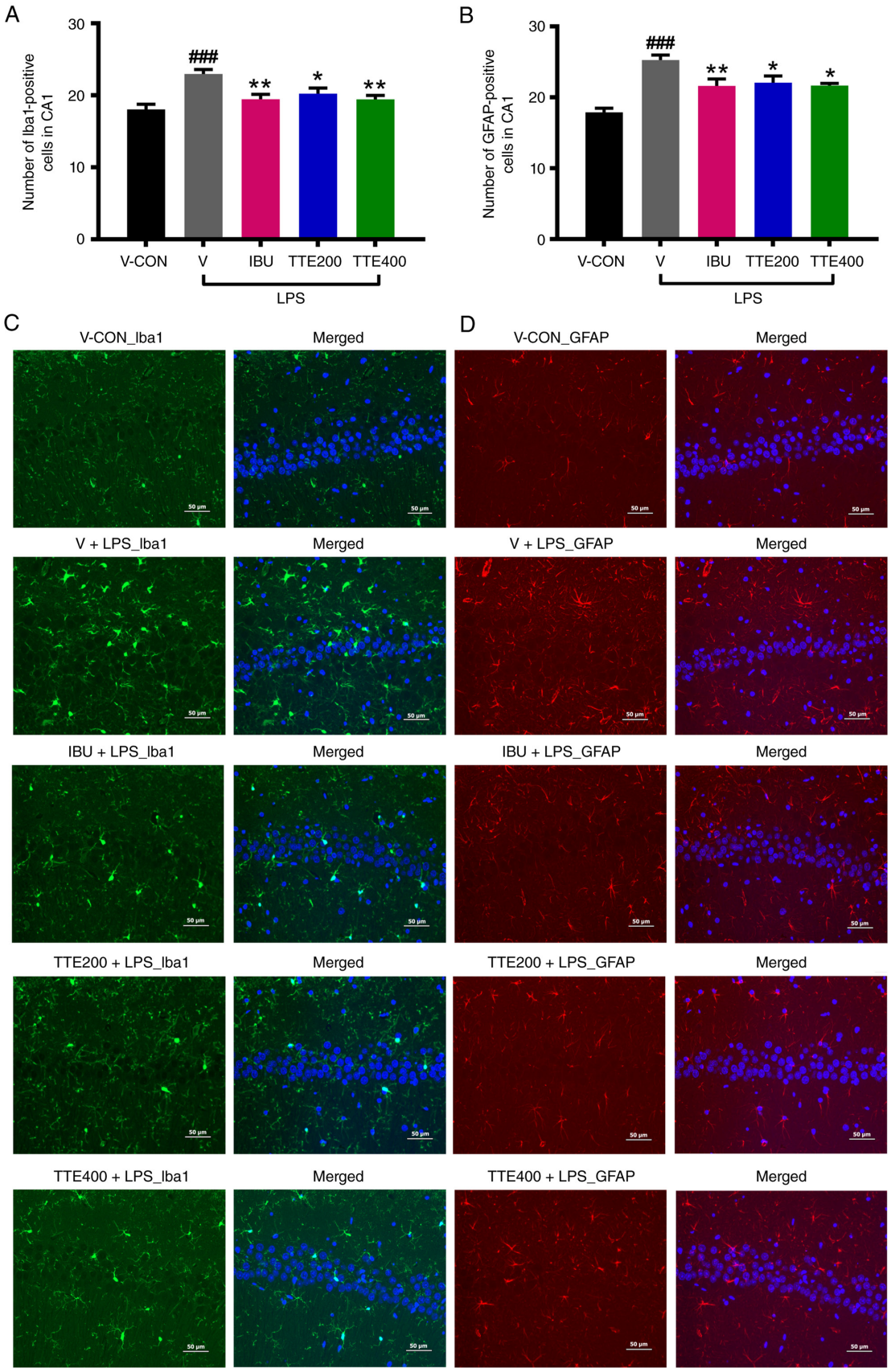

Figure 6. Effect of TTE on the number of Iba1- and GFAP-positive cells in the CA1. Number of (A) Iba1- and (B) GFAP-positive cells. The immunofluorescence of (C) Iba1-positive cells (green) and (D) GFAP-positive cells (red) in the CA1. Hoechst 33258 (blue) labels the nuclei of all cell types, including neurons and glial cells. Hippocampal neurons are characterized by larger, diffusely stained nuclei arranged in a dense and organized laminar pattern. The glial cells (microglia and astrocytes) exhibit smaller, intensely stained (punctate) nuclei that co-localize with Iba1 or GFAP immunoreactivity (43,44). The images were captured at 20x magnification (scale bar, 50 μm). One-way ANOVA was used to analyze the data, and the data is presented as the mean ± SEM (n=6). $^{###}$P<0.001 vs. the V-CON group. *P<0.05 and **P<0.01 vs. the V plus LPS group. TTE, *T. triandra* leaf extract; LPS, lipopolysaccharide; V-CON, vehicle-control; V, vehicle; IBU, ibuprofen; CA1, cornu ammonis 1; Iba1, ionized calcium-binding adapter molecule 1; GFAP, glial fibrillary acidic protein.

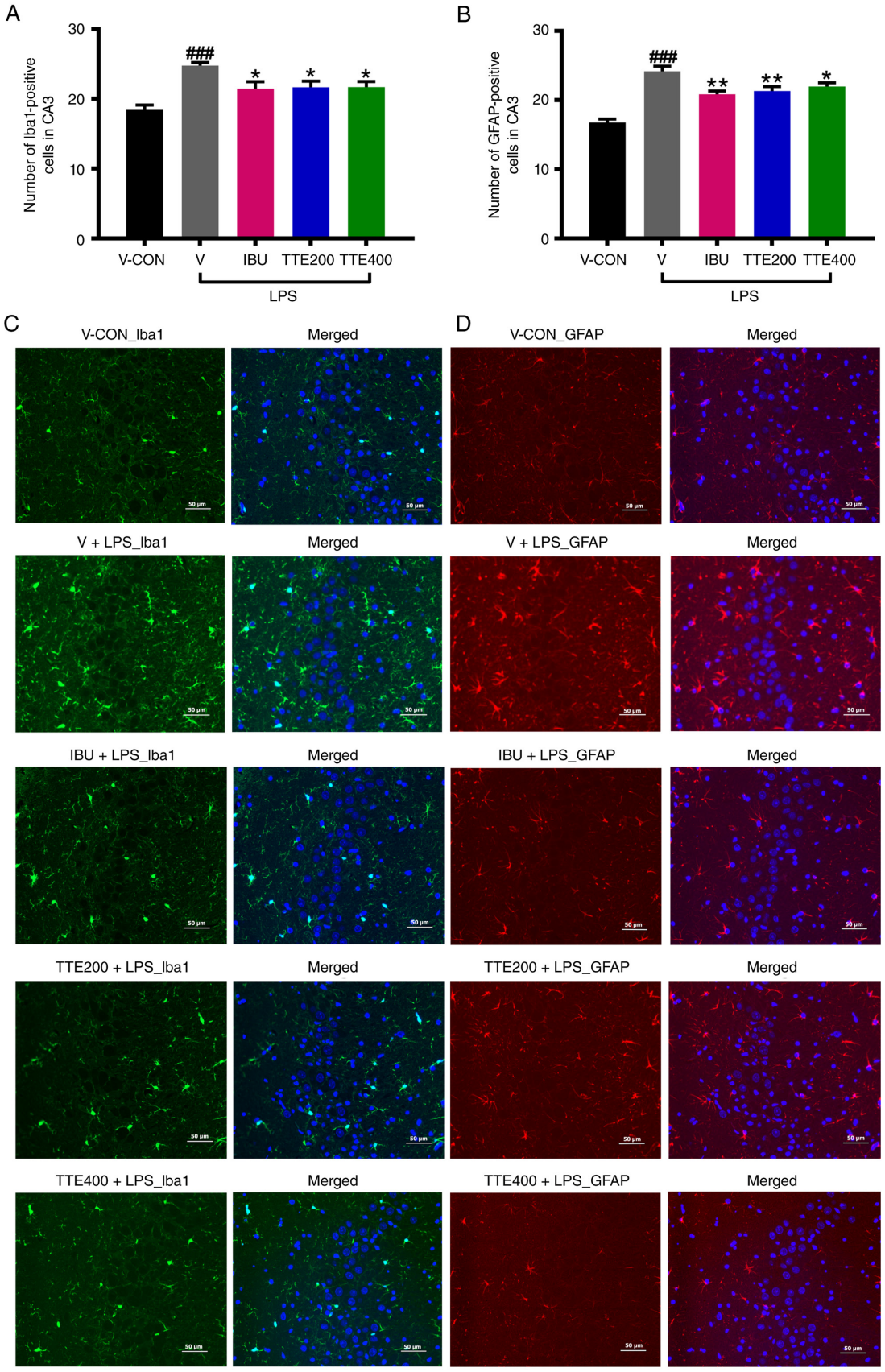

Figure 7. Effect of TTE on the number of Iba1- and GFAP-positive cells in the CA3. Number of (A) Iba1- and (B) GFAP-positive cells. The immunofluorescence of (C) Iba1-positive cells (green) and (D) GFAP-positive cells (red) in the CA3. Hoechst 33258 (blue) labels the nuclei of all cell types, including neurons and glial cells. Hippocampal neurons are characterized by larger, diffusely stained nuclei arranged in a dense and organized laminar pattern. The glial cells (microglia and astrocytes) exhibit smaller, intensely stained (punctate) nuclei that co-localize with Iba1 or GFAP immunoreactivity (43,44). The images were captured at 20x magnification (scale bar, 50 μm). One-way ANOVA was used to analyze the data, and the data is presented as the mean ± SEM (n=6). $^{###}$P<0.001 vs. the V-CON group. *P<0.05 and **P<0.01 vs. the V plus LPS group. TTE, *T. triandra* leaf extract; LPS, lipopolysaccharide; V-CON, vehicle-control; V, vehicle; IBU, ibuprofen; CA3, cornu ammonis 3; Iba1, ionized calcium-binding adapter molecule 1; GFAP, glial fibrillary acidic protein.

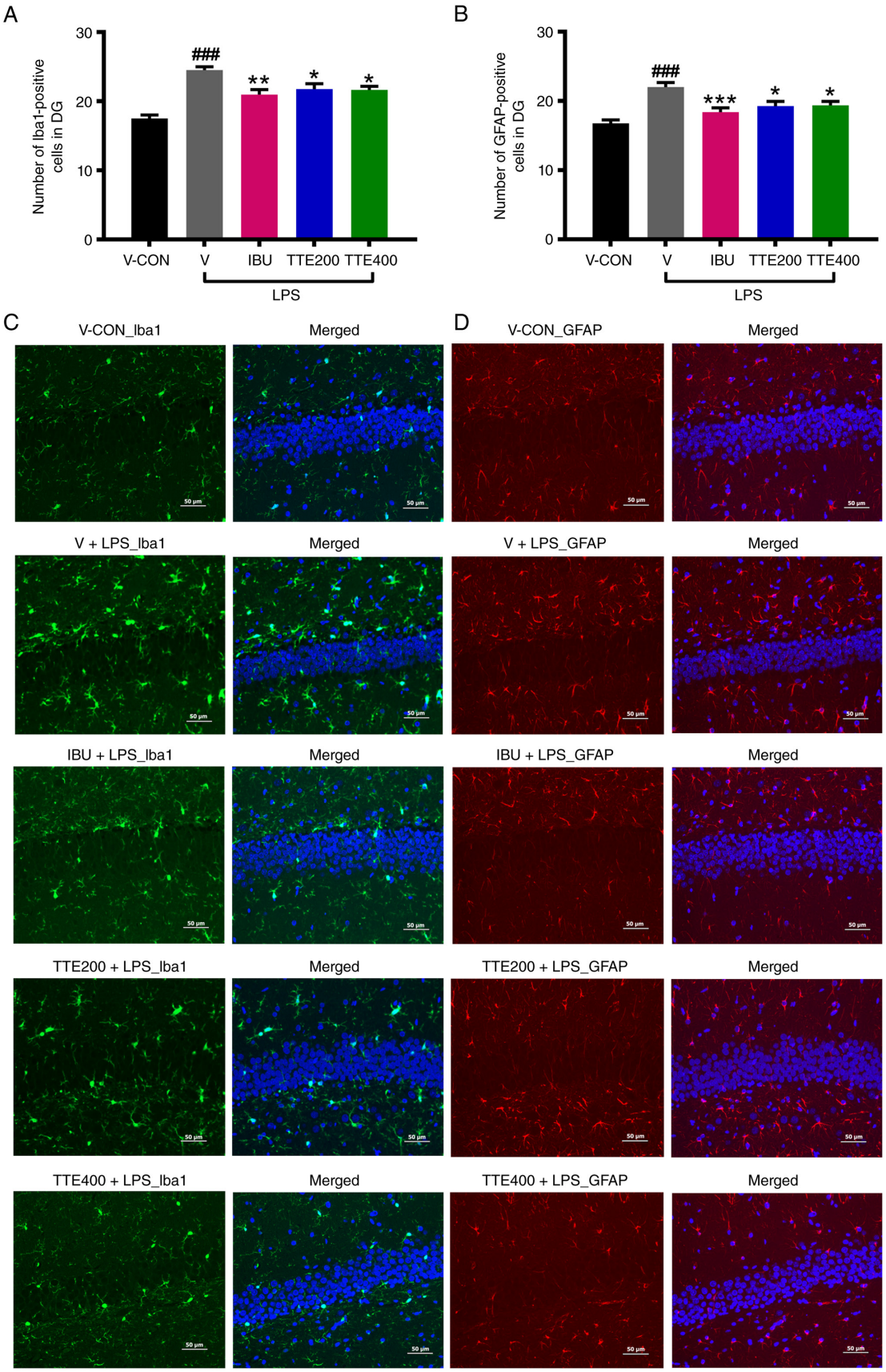

Figure 8. Effect of TTE on the number of Iba1- and GFAP-positive cells in the DG. Number of (A) Iba1- and (B) GFAP-positive cells. The immunofluorescence of (C) Iba1-positive cells (green) and (D) GFAP-positive cells (red) in the DG. Hoechst 33258 (blue) labels the nuclei of all cell types, including neurons and glial cells. Hippocampal neurons are characterized by larger, diffusely stained nuclei arranged in a dense and organized laminar pattern. The glial cells (microglia and astrocytes) exhibit smaller, intensely stained (punctate) nuclei that co-localize with Iba1 or GFAP immunoreactivity (43,44). The images were captured at 20x magnification (scale bar, 50 μm). One-way ANOVA was used to analyze the data, and the data is presented as the mean ± SEM (n=6). $^{###}$P<0.001 vs. the V-CON group. *P<0.05, **P<0.01 and ***P<0.001 vs. the V plus LPS group. TTE, *T. triandra* leaf extract; LPS, lipopolysaccharide; V-CON, vehicle-control; V, vehicle; IBU, ibuprofen; DG, dentate gyrus; Iba1, ionized calcium-binding adapter molecule 1; GFAP, glial fibrillary acidic protein.

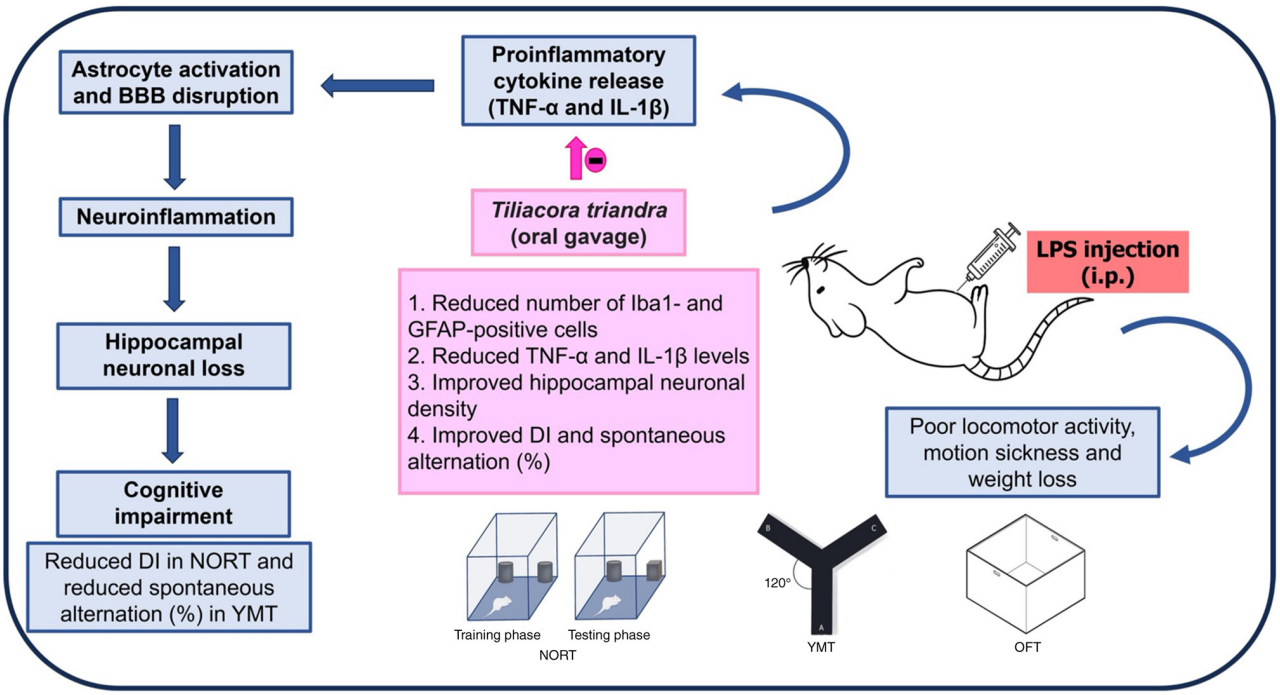

Figure 9. Proposed mechanisms of the possible neuroprotective actions of TTE against neuroinflammation and cognitive impairment. TTE may exert neuroprotective effects by reducing neuroinflammation and supporting neuronal survival. It lowers the levels of proinflammatory cytokines and suppresses microglial and astrocyte activation, as evidenced by reduced Iba1- and GFAP-positive cells in the hippocampus, which reduced inflammation-induced damage. These effects potentially contribute to improved cognitive function and reduced sickness-like behavior, suggesting its therapeutic potential for neuroinflammatory and memory-related disorders. LPS, lipopolysaccharide; GFAP, glial fibrillary acidic protein; Iba1, ionized calcium-binding adapter molecule 1; TNF-α, tumor necrosis factor-α; IL-1β, interleukin-1β; BBB, blood-brain barrier; YMT, Y-maze test; NORT, novel object recognition test; OFT, open field test; DI, discrimination index; i.p., intraperitoneal injection.

Discussion

The present study indicated that TTE may mitigate the LPS-induced cognitive impairments and neuroinflammation in rats. Compared with animals treated with vehicle plus LPS alone, animals treated with LPS plus TTE (at 200 or 400 mg/kg BW) had reduced expression levels of proinflammatory cytokines, including TNF-α and IL-1β, and decreased glial activation, as shown by reduced numbers of Iba1- and GFAP-positive cells. Neuronal density was also increased in LPS plus TTE treated animals compared with vehicle plus LPS treated animals, which may support neuronal function and contribute to neuroprotection. Overall, the findings of the present study suggested that TTE may potentially preserve cognitive function by mitigating neuroinflammation.

LPS, a component of the outer membrane of Gram-negative bacteria, is widely used to induce systemic or CNS inflammation in experimental models (16). In the present study, the LPS administration protocol was designed to produce subacute neuroinflammation as opposed to chronic neurotoxicity. The 7-day regimen of daily intraperitoneal injections of LPS (250 μg/kg BW) is commonly used to generate sustained systemic inflammation that leads to neuroinflammatory responses and cognitive impairment without progressing to long-term neurodegeneration, as reported in previous studies (34,35). Peripheral LPS exposure disrupts physiological and behavioral functions, causing weight loss, sickness behavior and cognitive deficits (16,17). These outcomes are mostly induced by elevated proinflammatory cytokines and disturbances in hippocampal neural processes (17). Consistent with previous findings, animals injected with LPS for 7 days showed a significant reduction in BW, locomotor activity and cognitive performance, as indicated by a reduced discrimination index in the NORT and reduced spontaneous alternations in the YMT. Co-treatment with TTE (at 200 or 400 mg/kg BW) improved both cognitive and locomotor outcomes, which was further supported by an enhanced performance in the OFT. These findings align with previous reports showing that repeated LPS exposure at comparable doses induces cognitive dysfunction and behavioral disturbances, including reduced food intake, BW and exploratory behavior (50,51).

Neuroinflammation is an immune response in the CNS induced by triggers such as infection, injury or neurodegeneration. It is characterized by the activation and proliferation of glial cells, particularly microglia and astrocytes, which sustain inflammatory signaling (7,8). Microglia respond to stimuli such as LPS by shifting to a proinflammatory state and increasing in number, which is reflected by elevated Iba1 expression levels. These activated microglia release cytokines, including TNF-α and IL-1β, contributing to neuronal dysfunction (50-52). In the present study, LPS-treated animals receiving TTE showed significantly reduced TNF-α and IL-1β levels compared with LPS-treated animals receiving vehicle, which aligns with previous work (19) demonstrating that the components of TTE may exert effects through the suppression of pathways such as NF-κB (19). TTE also decreases iNOS and COX-2 expression levels in LPS-stimulated macrophages (20,21). The regulation of iNOS-derived NO is mechanistically important because NO

can either suppress or promote inflammation, and it directly influences heme-dependent enzymes (including cytochrome P450) through concentration-dependent effects on heme availability and enzymatic activity (53). These findings support the anti-inflammatory and neuroprotective actions of TTE.

LPS-induced neuroinflammation is characterized by the activation of both microglia and astrocytes. Microglial activation, marked by an increased expression of Iba1, leads to the release of proinflammatory cytokines and ROS, while astrocytes undergo reactive astrogliosis, reflected as elevated GFAP levels and increased production of inflammatory mediators (7,8). Sustained activation of these glial cells reinforces chronic neuroinflammation and contributes to neural dysfunction. In the present study, 7 days of LPS administration significantly elevated Iba1- and GFAP-positive cell populations within the hippocampus, consistent with previous reports demonstrating LPS-induced gliosis at similar doses (17,50,51). Co-treatment of LPS with TTE markedly reduced the number of both Iba1- and GFAP-positive cells, indicating that TTE attenuates LPS-induced neuroinflammatory responses. Similar anti-inflammatory activity is reported for the Thai herbal Ha-Rak Formula, which contains TTE, and is shown to decrease TNF-α, IL-1β and IL-6 levels in LPS-induced systemic inflammation (52).

Neuronal density, a key indicator of hippocampal structural integrity and functional capacity, is vulnerable to glial-mediated inflammation (54). Elevated GFAP and Iba1 expression levels is associated with neuronal loss across neurodegenerative models, including AD, PD and LPS-induced neuroinflammation (46,50,55). In the present study, LPS exposure led to a significant reduction in neuronal density within the CA1, CA3 and DG regions, supporting the association between prolonged neuroinflammation, synaptic dysfunction and cognitive impairment. However, LPS exposure with TTE treatment significantly restored neuronal density in these hippocampal subfields, aligning with previous findings demonstrating that TTE enhances cholinergic function, promotes neuronal density and improves memory performance across multiple hippocampal regions (22,24).

The findings of the present study indicated that TTE induced effects that were comparable to those of the positive control, IBU. Whereas IBU primarily exerts its effects through COX inhibition, TTE appears to modulate multiple downstream pathways, including reductions in proinflammatory cytokine levels and glial activation, as well as improvements in neuronal density (33,56). Although the present study did not establish the sequence or hierarchy of these mechanisms, the broader spectrum of effects observed with TTE suggested that its neuroprotective actions may extend beyond classical anti-inflammatory activity. In addition, TTE exerts antioxidant effects, enhances cholinergic functions and ameliorates 1-methyl-4-phenyl-1,2,3,6-tetrahydropyridine (MPTP)-induced motor impairment (22-24,57). TTE also attenuates MPTP-induced reductions in tyrosine hydroxylase-positive neurons in the substantia nigra and mitigates decreases in striatal dopamine levels (23). Moreover, TTE protects against oxidative stress by reducing malondialdehyde levels and modulating catalase (CAT), superoxide dismutase (SOD), and reduced glutathione, while also decreasing brain infarction and histopathological alterations in the cerebral cortex and hippocampus in a mouse model of cerebral ischemia-reperfusion (25). Furthermore, TTE induces the expression of antioxidant enzymes, including copper-zinc SOD (Cu-ZnSOD), glutathione peroxidase and CAT. In addition to its neuroprotective effects, TTE decreases hepatic glucose production by downregulating phosphoenolpyruvate carboxykinase and glucose-6-phosphatase and by increasing protein kinase B and AMP-activated protein kinase phosphorylation in HepG2 cells. These molecular effects are associated with the antihyperglycemic, anti-triglyceridemic, anti-insulin resistance and antioxidant activities of TTE observed in type 2 diabetes mellitus rat models, which is comparable to those achieved with metformin and combination treatments (58). Overall, the magnitude of the effects induced by TTE are comparable to those induced by IBU, supporting the suggestion that TTE may function as a multi-target therapeutic agent as opposed to solely as an anti-inflammatory compound. This comparison indicates the possible therapeutic potential of TTE and highlights its potentially broader pharmacological profile relative to the single-target mechanism of IBU.

In the present study, the quantitative analysis of the polyphenolic constituents revealed a clear contrast between the TFC and TPC of TTE. The extract showed a high flavonoid concentration (30.08 mg QE/g extract), whereas the level of compounds reactive to the Folin-Ciocalteu reagent was low (0.020 mg GAE/g extract). This finding was unusual because flavonoids are chemically classified as phenolic compounds; therefore, the TPC value was expected to be equal to or greater than the TFC value. These results indicated that flavonoids were the dominant polyphenolic constituents of TTE, while Folin-reactive phenolic acids or gallic acid were present only at minimal levels. This phytochemical profile may influence the biological properties of TTE, as flavonoids are well known for their antioxidant and anti-inflammatory activities (59-61). However, the low TPC value also highlighted the limitations of relying solely on the Folin-Ciocalteu assay to characterize complex plant extracts. Complementary analytical methods, such as high-performance liquid chromatography (HPLC) profiling or antioxidant assays that directly assess radical scavenging capacity, may provide a more comprehensive understanding of the phytochemical composition and bioactivity of TTE.

Taken together, the TTE used in the present study potentially contained high levels of flavonoids that may have exerted neuroprotective effects through multiple complementary mechanisms. The anti-inflammatory activity of TTE, suggested by reduced cytokine levels and the number of both Iba1- and GFAP-positive cells (likely mediated through suppression of NF-κB signaling (19), aligned with previous reports showing that TTE decreases iNOS and COX-2 expression levels in LPS-stimulated macrophages (20,21), leading to reduced TNF-α, IL-1β and IL-6 levels in models of rats with LPS-induced systemic inflammation (52). TTE may also support neuronal integrity by enhancing neuronal density (22-24) and improving cholinergic function, which is indicated by increases in choline acetyltransferase expression levels (57) and inhibition of acetylcholinesterase activity (22,24), which together may contribute to improved cognitive performance. In addition, its antioxidant properties,

demonstrated by reduced oxidative stress markers and increased antioxidant enzyme activities (22-25), along with potential neurotrophic effects, may further promote neuronal preservation and functional resilience. Collectively, these findings indicate mechanistic support for the anti-inflammatory and neuroprotective actions of TTE, highlighting its therapeutic potential in mitigating LPS-induced glial activation and cognitive impairment. These proposed mechanisms are summarized in Fig. 9.

However, the present study did not reveal a clear dose-response association between the 200 and 400 mg/kg doses of TTE across several endpoints. One possibility is that 200 mg/kg may have already produced a near-maximal pharmacodynamic effect, so that increasing the dose to 400 mg/kg yielded little additional benefit. Non-linear pharmacokinetics or limited bioavailability at higher doses may also have restricted further tissue exposure. In addition, receptor or pathway saturation and downstream bottlenecks could have capped the biological response, while metabolic induction or enhanced clearance at the higher dose may have reduced incremental effects. Future work should include pharmacokinetic assessments and pathway-specific or time-course assays in order to capture transient or dose-dependent signaling changes.

The present study had several limitations. Firstly, the use of a crude herbal extract introduced inherent variability, and the lack of quantitative phytochemical characterization (such as with HPLC fingerprinting) limited the ability of the present study to associate specific constituents with the observed biological effects. Secondly, although the LPS-induced rodent model is widely used to investigate neuroinflammation, it was a subacute inflammatory state and did not fully capture the chronic and progressive characteristics of human neurodegenerative diseases. Thirdly, although the use of six animals per group aligned with standard practice in rodent studies, this sample size was at the lower end for achieving strong statistical power, which increased the risk of type II errors. Therefore, subtle or moderate effects may have gone undetected, and future studies using larger cohorts are needed to enhance statistical reliability and reproducibility. Finally, mechanistic uncertainties persist, particularly regarding the potential involvement of specific molecular targets and downstream pathways such as NF-κB signaling and the expression of COX-2, highlighting the need for pathway-specific assays to clarify the molecular mechanisms underlying the observed neuroprotective effects.

In conclusion, the findings of the present study indicated that TTE may induce significant neuroprotective effects in an LPS-induced model of neuroinflammation potentially by attenuating neuronal loss and suppressing glial activation. This neuroprotection was suggested due to the downregulation of proinflammatory cytokines and a reduced number of Iba1- and GFAP-positive glial cells. These molecular and cellular changes were associated with improved cognitive function and increased neuronal density. Collectively, these results suggested that TTE may be a potential therapeutic agent for alleviating neuroinflammation and cognitive deficits that are associated with neurodegenerative and inflammatory conditions.

Acknowledgements

Not applicable.

Funding

This work was supported by Mae Fah Luang University, Thailand Science Research and Innovation, and National Science, Research and Innovation Fund, under the Fundamental Fund 2025 (grant no. 682A07012).

Availability of data and materials

The data generated in the present study may be requested from the corresponding author.

Authors' contributions

NS was involved in the conception and design of the present study, execution of experiments, curation and analysis of data, writing of the original draft, as well as the review and editing of the manuscript. SP, UK and AW were involved in the execution of experiments, the animal study and obtaining resources. SA was involved in the execution of experiments, obtaining resources, retrieval, curation and analysis of the data, and writing the original draft. PI was involved in the execution of experiments, retrieval, curation and analysis of the data, and reviewing and editing the manuscript. TH was involved in the conception and design of the present study, funding acquisition, execution of experiments, the animal study, curation and analysis of the data, visualization, writing of the original draft, manuscript review and editing, and project administration. NS and TH confirm the authenticity of all the raw data. All authors read and approved the final version of the manuscript.

Ethics approval and consent to participate

The experiment received approval from the Ethics Committee of the Laboratory Animal Research Center of Mae Fah Luang University (approval no. AR04/67; Chiang Rai, Thailand).

Patient consent for publication

Not applicable.

Competing interests

The authors declare that they have no competing interests.

References

1. Adamu A, Li S, Gao F and Xue G: The role of neuroinflammation in neurodegenerative diseases: Current understanding and future therapeutic targets. Front Aging Neurosci 16: 1347987, 2024.
2. Kwon HS and Koh SH: Neuroinflammation in neurodegenerative disorders: The roles of microglia and astrocytes. Transl Neurodegener 9: 42, 2020.
3. Pekny M, Pekna M, Messing A, Steinhäuser C, Lee JM, Parpura V, Hol EM, Sofroniew MV and Verkhratsky A: Astrocytes: A central element in neurological diseases. Acta Neuropathol 131: 323-345, 2016.
4. Liddelow SA and Barres BA: Reactive astrocytes: Production, function, and therapeutic potential. Immunity 46: 957-967, 2017.

5. Rizzo FR, Musella A, De Vito F, Fresegna D, Bullitta S, Vanni V, Guadalupi L, Stampanoni Bassi M, Buttari F, Mandolesi G, *et al*: Tumor necrosis factor and interleukin-1β modulate synaptic plasticity during neuroinflammation. Neural Plast 2018: 8430123, 2018.
6. DiSabato DJ, Quan N and Godbout JP: Neuroinflammation: The devil is in the details. J Neurochem 139 (Suppl 2): S136-S153, 2016.
7. Pekny M and Pekna M: Astrocyte reactivity and reactive astrogliosis: Costs and benefits. Physiol Rev 94: 1077-1098, 2014.
8. Lier J, Streit WJ and Bechmann I: Beyond activation: Characterizing microglial functional phenotypes. Cells 10: 2236, 2021.
9. Wang C, Zong S, Cui X, Wang X, Wu S, Wang L, Liu Y and Lu Z: The effects of microglia-associated neuroinflammation on Alzheimer's disease. Front Immunol 14: 1117172, 2023.
10. Spangenberg EE and Green KN: Inflammation in Alzheimer's disease: Lessons learned from microglia-depletion models. Brain Behav Immun 61: 1-11, 2017.
11. Heneka MT, Carson MJ, El Khoury J, Landreth GE, Brosseron F, Feinstein DL, Jacobs AH, Wyss-Coray T, Vitorica J, Ransohoff RM, *et al*: Neuroinflammation in Alzheimer's disease. Lancet Neurol 14: 388-405, 2015.
12. Winner B and Winkler J: Adult neurogenesis in neurodegenerative diseases. Cold Spring Harb Perspect Biol 7: a021287, 2015.
13. Ransohoff RM: How neuroinflammation contributes to neurodegeneration. Science 353: 777-783, 2016.
14. Dabi YT, Ajagbe AO and Degechisa ST: Toll-like receptors in pathogenesis of neurodegenerative diseases and their therapeutic potential. Immun Inflamm Dis 11: e839, 2023.
15. Muzio L, Viotti A and Martino G: Microglia in neuroinflammation and neurodegeneration: From understanding to therapy. Front Neurosci 15: 742065, 2021.
16. Zhao J, Bi W, Xiao S, Lan X, Cheng X, Zhang J, Lu D, Wei W, Wang Y, Li H, *et al*: Neuroinflammation induced by lipopolysaccharide causes cognitive impairment in mice. Sci Rep 9: 5790, 2019.
17. Choe K, Park JS, Park HY, Tahir M, Park TJ and Kim MO: Lupeol protect against LPS-induced neuroinflammation and amyloid beta in adult mouse hippocampus. Front Nutr 11: 1414696, 2024.
18. Zhang X, Peng X, Wang C, Olatunji OJ and Famurewa A: *Tiliacora triandra* attenuates cisplatin triggered hepatorenal and testicular toxicity in rats by modulating oxidative inflammation, apoptosis and endocrine deficit. Front Biosci (Landmark Ed) 27: 44, 2022.
19. Huang Y, Liu C, Song X, An M, Liu M, Yao L, Famurewa AC and Olatunji OJ: Antioxidant and anti-inflammatory properties mediate the neuroprotective effects of hydro-ethanolic extract of *Tiliacora triandra* against cisplatin-induced neurotoxicity. J Inflamm Res 14: 6735-6748, 2021.
20. Weerawatanakorn M, Rojsuntornkitti K, Pan MH and Wongwaiwech D: Some phytochemicals and anti-inflammation effect of juice from *Tiliacora triandra* leaves. J Food Nutr Res 6: 32-38, 2018.
21. Pradubyat N, Wunnakup T, Praparatana R, Wongwiwatthananukit S, Jongrungruangchok S, Songsak T, Madaka F and Sudsai T: Evaluation of antioxidant and anti-inflammatory properties, bioactive compound profiling, and molecular mechanisms of a multicomponent Thai herbal formulation. Phytomed Plus 4: 100662, 2024.
22. Hawiset T, Sriraksa N, Kamsrijai U, Praman S and Inkaew P: Neuroprotective effect of *Tiliacora triandra* (Colebr.) Diels leaf extract on scopolamine-induced memory impairment in rats. Heliyon 9: e22545, 2023.
23. Sriraksa N, Hawiset T, Kongsui R, Thongrong S, Promsrisuk T and Boontem P: *Tiliacora triandra* (Colebr.) Diels leaf extract alleviates motor deficit and protects against MPTP-induced neurodegeneration in mice. J Appl Pharm Sci 14: 230-237, 2024.
24. Phunchago N, Wattanathorn J and Chaisiwamongkol K: *Tiliacora triandra*, an anti-intoxication plant, improves memory impairment, neurodegeneration, cholinergic function, and oxidative stress in hippocampus of ethanol dependence rats. Oxid Med Cell Longev 2015: 918426, 2015.
25. Thong-Asa W and Bullangpoti V: Neuroprotective effects of *Tiliacora triandra* leaf extract in a mice model of cerebral ischemia reperfusion. Avicenna J Phytomed 10: 202-212, 2020.
26. Kumar N and Chaiyasut C: Health promotion potential of vegetables cultivated in Northern Thailand: A preliminary screening of tannin and flavonoid contents, 5α-reductase inhibition, astringent activity, and antioxidant activities. J Evid Based Complementary Altern Med 22: 573-579, 2017.
27. Faul F, Erdfelder E, Lang AG and Buchner A. G*Power 3: A flexible statistical power analysis program for the social, behavioral, and biomedical sciences. Behav Res Methods 39: 175-191, 2007.
28. Faul F, Erdfelder E, Buchner A and Lang AG: Statistical power analyses using G*Power 3.1: Tests for correlation and regression analyses. Behav Res Methods 41: 1149-1160, 2009.
29. University of Arizona: Guidelines for Anesthetic and Analgesic Use in Laboratory Animals. https://www.spandidos-publications.com/var/GuidelinesAnestheticAnalgesicUse.pdf. Accessed January, 2026.
30. American Veterinary Medical Association: AVMA guidelines for the euthanasia of animals: 2020 edition. AVMA, Schaumburg, IL, 2020.
31. Lucera GM, Menani JV, Colombari E and Colombari DSA: ANG II and aldosterone acting centrally participate in the enhanced sodium intake in water-deprived renovascular hypertensive rats. Front Pharmacol 12: 679985, 2021.
32. Sireeratawong S, Lertprasertsuke N, Srisawat U, Thuppia A, Ngamjariyawat A, Suwanlikhid N and Jaijoy K: Acute and subchronic toxicity study of the water extract from *Tiliacora triandra* (Colebr.) Diels in rats. Songklanakarin J Sci Technol 30: 611-619, 2008.
33. Nayak A, Raju R, Das P, Das K, Suvitha A, Ranjan Meher B, Alobid S, Almoteer AI, Almadani ME, Alshehri A, *et al*: Novel ibuprofen prodrug: A possible promising agent for the management of complications of Alzheimer's disease. Saudi Pharm J 32: 101888, 2024.
34. Thingore C, Kshirsagar V and Juvekar A: Amelioration of oxidative stress and neuroinflammation in lipopolysaccharide-induced memory impairment using Rosmarinic acid in mice. Metab Brain Dis 36: 299-313, 2021.
35. Ali W, Choe K, Park JS, Ahmad R, Park HY, Kang MH, Park TJ and Kim MO: Kojic acid reverses LPS-induced neuroinflammation and cognitive impairment by regulating the TLR4/NF-κB signaling pathway. Front Pharmacol 15: 1443552, 2024.
36. Blossom V, Ullal SD, Rai R, Chakraborthi S, Kumar NA, Pai MM and Vadgaonkar R: Bacterial lipopolysaccharide model of neuroinflammation-associated neurodegeneration in Wistar rats: A comparison between different durations of lipopolysaccharide induction. Vet World 17: 2567-2576, 2024.
37. Benmhammed H, Lamtai M, Mesfioui A, Nassiri A, Mouden S, Bikri S and Hessni AEl: Effects of lipopolysaccharide administration at different postnatal periods on behavioral and biochemical assessments in Wistar rats. Neurosci Behav Physiol 54: 357-373, 2024.
38. Onasanwo SA, Adebimpe-John OE, Olopade FE and Olajide OO: Kolaviron protects rats from cognitive decline induced by lipopolysaccharide in Wistar rat. Niger J Physiol Sci 36: 67-76, 2021.
39. Azzam SM, Abdel Rahman AAS, Ahmed-Farid OA, Abu El-Wafa WM and Salem GEM: Lipopolysaccharide induced neuroprotective effects of bacterial protease against Alzheimer's disease in male Wistar albino rats. Int J Biol Macromol 230: 123260, 2023.
40. Hawiset T, Sriraksa N, Anukanon S, Kamsrijai U, Praman S, Teerapattarakan N and Inkaew P: *Tacca chantrieri* André rhizome extract alleviates scopolamine-induced cognitive impairment and neuroinflammation in rats. Adv Pharmacol Pharm Sci 2025: 7334303, 2025.
41. Hawiset T, Sriraksa N, Kongsui R, Kamsrijai U, Wanchai K and Inkaew P: *Azadirachta indica* A. Juss. flower extract attenuated memory deficit-induced by restraint stress in male rats. Physiol Pharmacol 27: 53-63, 2023.
42. Hawiset T, Sriraksa N, Kamsrijai U, Wanchai K and Inkaew P: Anxiolytic and antidepressant-like activities of aqueous extract of *Azadirachta indica* A. Juss. flower in the stressed rats. Heliyon 8: e08881, 2022.
43. Cerbai F, Lana D, Nosi D, Petkova-Kirova P, Zecchi S, Brothers HM, Wenk GL and Giovannini MG: The neuron-astrocyte-microglia triad in normal brain ageing and in a model of neuroinflammation in the rat hippocampus. PLoS One 7: e45250, 2012.
44. García-Cabezas MÁ, John YJ, Barbas H and Zikopoulos B: Distinction of neurons, glia and endothelial cells in the cerebral cortex: An algorithm based on cytological features. Front Neuroanat 10: 107, 2016.

45. Skrzypczak-Wiercioch A and Sałat K: Lipopolysaccharide-induced model of neuroinflammation: Mechanisms of action, research application and future directions for its use. Molecules 27: 5481, 2022.
46. Fołta J, Rzepka Z and Wrześniok D: The role of inflammation in neurodegenerative diseases: Parkinson's disease, Alzheimer's disease, and multiple sclerosis. Int J Mol Sci 26: 5177, 2025.
47. Kongsui R, Promsrisuk T, Chanmanee T, Klimaschewski L, Jamsuwan S, Sriraksa N, Jittiwat J and Thongrong S: Biochanin A prevents neurodegeneration and oxidative stress in a kainic acid model of epilepsy by activating the PI3K/Akt/Nrf2 signaling pathway. Sci Rep 15: 39842, 2025.
48. Zhang L, Li J and Lin A: Assessment of neurodegeneration and neuronal loss in aged 5XFAD mice. STAR Protoc 2: 100915, 2021.
49. Palachai N, Supawat A, Kongsui R, Klimaschewski L and Jittiwat J: Galangin's neuroprotective role: Targeting oxidative stress, inflammation, and apoptosis in ischemic stroke in a rat model of permanent middle cerebral artery occlusion. Int J Mol Sci 26: 1847, 2025.
50. Khan MS, Ali T, Kim MW, Jo MH, Jo MG, Badshah H and Kim MO: Anthocyanins protect against LPS-induced oxidative stress-mediated neuroinflammation and neurodegeneration in the adult mouse cortex. Neurochem Int 100: 1-10, 2016.
51. Lee JW, Lee YK, Yuk DY, Choi DY, Ban SB, Oh KW and Hong JT: Neuro-inflammation induced by lipopolysaccharide causes cognitive impairment through enhancement of beta-amyloid generation. J Neuroinflammation 5: 37, 2008.
52. Booranasubkajorn S, Kanlaya H, Huabprasert S, Lumlerdkij N, Akarasereenont P and Tripatara P: The effect of Thai herbal Ha-Rak Formula (HRF) on LPS-induced systemic inflammation in Wistar rats. Siriraj Med J 69: 356-362, 2017.
53. Das Sinha P, Islam S, Biswas P and Stuehr DJ: Nitric oxide regulates cytochrome P450 2D6 and 3A4 activity via concentration-dependent modulation of heme loading. J Biol Chem 301: 110772, 2025.
54. Rozhkova IN, Okotrub SV, Brusentsev EY, Uldanova EE, Chuyko EA, Lipina TV, Amstislavskaya TG and Amstislavsky SY: Neuronal density in the brain cortex and hippocampus in Clsnt2-KO mouse strain modeling autistic spectrum disorder. Vavilovskii Zhurnal Genet Selektsii 26: 365-370, 2022.
55. Lawrence JM, Schardien K, Wigdahl B and Nonnemacher MR: Roles of neuropathology-associated reactive astrocytes: A systematic review. Acta Neuropathol Commun 11: 42, 2023.
56. Rainsford KD: Ibuprofen: Pharmacology, efficacy and safety. Inflammopharmacology 17: 275-342, 2009.
57. Wachiryah TA and Hathaipat L: Enhancing effect of *Tiliacora triandra* leaves extract on spatial learning, memory and learning flexibility as well as hippocampal choline acetyltransferase activity in mice. Avicenna J Phytomed 8: 380-388, 2018.
58. Pasachan T, Duangjai A, Ontawong A, Amornlerdpison D, Jinakote M, Phatsara M, Soodvilai S and Srimaroeng C: *Tiliacora triandra* (Colebr.) Diels leaf aqueous extract inhibits hepatic glucose production in HepG2 cells and type 2 diabetic rats. Molecules 26: 1239, 2021.
59. Al-Khayri JM, Sahana GR, Nagella P, Joseph BV, Alessa FM and Al-Mssallem MQ: Flavonoids as potential anti-inflammatory molecules: A review. Molecules 27: 2901, 2022.
60. Zahra M, Abrahamse H and George BP: Flavonoids: Antioxidant powerhouses and their role in nanomedicine. Antioxidants (Basel) 13: 922, 2024.
61. Navarro-Hoyos M, Bisoyi R, Kc P, Lutz N and Ruxsarash M: Key dietary flavonoids: Insights into their structural characteristics, antioxidant and anti-inflammatory activities, and potential as neuroprotective agents. Molecules 31: 154, 2026.